NON-CONTACT FLUORESCENCE OPTICAL TOMOGRAPHY WITH SCANNING AREA ILLUMINATION

Amit Joshi,[1] *Wolfgang Bangerth,*[2] *and Eva M. Sevick-Muraca*[1*]

[1]Department of Radiology, Baylor College of Medicine, Houston, Texas 77030
[2] Department of Mathematics, Texas A & M University, College Station, TX 77840

ABSTRACT

This contribution describes a novel non-contact fluorescence optical tomography scheme which utilizes multiple area illumination patterns, to reduce the illposedness of the inverse problem involved in recovering interior fluorescence yield distribution in biological tissue from boundary fluorescence measurements. Multiple excitation source illumination patterns are simulated by gaussian beam sources scanning the simulated tissue phantom surface. Area measurements of fluorescence amplitude and phase are collected on the illumination plane. Multiple measurement data sets generated by scanning the excitation sources are processed simultaneously to generate the interior fluorescence distribution in tissue by implementing a dual adaptive finite element based fluorescence tomography algorithm in a parallel framework suitable for multiprocessor computers. Image reconstructions for multiple fluorescent targets ($5mm$ diameter) embedded in a $512ml$ simulated tissue phantom are demonstrated.

1. INTRODUCTION

Fluorescence optical tomography is one of several active areas in molecular imaging research. The objective of fluorescence optical tomography is to recover the interior fluorescence yield or lifetime distributions in tissue media from boundary measurements of fluorescence emission generated by the excitation light delivered to the tissue boundary. The recovery of the true interior fluorophore distribution is contingent on the information content of the boundary fluorescence measurements, which can be enhanced by employing a wide spatial placement of boundary excitation sources and detectors. Typically this is performed by using multiple fiber optics for delivering excitation light via direct contact with tissue or by mechanically raster scanning a focused laser [1, 2], and taking fluorescence measurements at different locations on the tissue boundary. However point illumination based tomography systems suffer from sparse measurement data sets, and inadequate amount of excitation light penetration in the tissue interior, especially for imaging clinically relevant tissue volumes. In the past, researchers at the Photon Migration Laboratories have demonstrated area-illumination and area-detection based fluorescence tomography approaches, wherein excitation light is delivered to the tissue media by expanding a laser beam over the tissue surface, and fluorescence measurements are taken on the illumination surface by an intensified CCD camera system [3]. While area-illumination provides enhances excitation light penetration, the tomography problem is hard to solve because of the increased illposedness introduced by the availability of only the reflectance measurements for inversion. The information content in the area measurements can be increased by employing spatially varying or patterned illumination, and taking multiple reflectance measurements corresponding to different illumination patterns. This task can be performed by focusing multiple Gaussian excitation source patterns on different locations on the tissue phantom, resulting in a non-contact analogue of traditional point illumination based measurements, but with enhanced tissue surface coverage per excitation source (Fig-1). Model based tomography in an area illumination and detection framework requires accurate numerical solution of the photon fluence distribution in the tissue created by spatially patterned illumination sources. In the past, we have demonstrated an efficient adaptive finite element tomography algorithm to solve plane wave excitation fluorescence tomography problem [4]. Herein, we extend that approach to handle multiple spatially patterned illumination sources. Adaptive finite element based numerical solutions are implemented for multiple area sources independently of each other on separate finite element meshes, which adapt to accurately resolve each excitation source. Information from multiple measurements is combined to update the unknown interior fluorescence distribution in tissue. The proposed scheme is optimized for parallel cluster computers, as the adaptive finite element solvers for different source patterns can run on different processors. The formulation and implementation of the proposed fluorescence tomography scheme are detailed in section-2. The image reconstructions from multiple area illumination patterns are presented in section-3. We conclude this article in section-4 by detailing the advantages gained by employing multiple area illumination patterns and the future implications for clinical fluorescence imaging.

*Thanks to NIH grant no. RO1 CA112679 for funding.

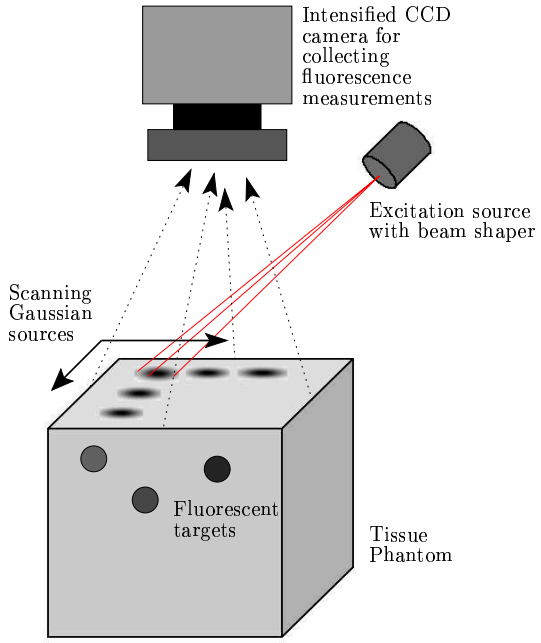

Fig. 1. Illustration of scanning gaussian source based excitation illumination.

2. METHODS AND FORMULATION

Fluorescence optical tomography is typically performed in a model-based framework, wherein a photon transport model is used to generate predicted boundary fluorescence measurements for a given fluorescence absorption map in the tissue interior. The map of the absorption owing to fluorophore is then iteratively updated until the predicted boundary fluorescence measurements converge to the actual experimentally observed fluorescence measurements. For time dependent photon propagation in large tissue volumes, the following set of coupled photon diffusion equations are an accurate model in frequency space:

$$-\nabla \cdot [D_x(\mathbf{r})\nabla u(\mathbf{r},\omega)] + k_x u(\mathbf{r},\omega) = 0, \quad (1)$$

$$-\nabla \cdot [D_m(\mathbf{r})\nabla v(\mathbf{r},\omega)] + k_m v(\mathbf{r},\omega) = \beta_{xm} u(\mathbf{r},\omega). \quad (2)$$

Here,

$$D_{x,m} = \frac{1}{3(\mu_{ax,mi} + \mu_{ax,mf} + \mu'_{sx,m})},$$

$$k_{x,m} = \frac{i\omega}{c} + \mu_{ax,mi}(\mathbf{r}) + \mu_{ax,mf}(\mathbf{r}), \beta_{xm} = \frac{\phi\mu_{axf}}{1 - i\omega\tau(\mathbf{r})},$$

and subscripts x and m denote the excitation and the emission light fields, respectively. u, v are the complex-valued photon fluence fields at excitation and emission wavelengths, respectively; $D_{x,m}$ are the photon diffusion coefficients; $\mu_{ax,mi}$ is the absorption coefficient due to endogenous chromophores; $\mu_{ax,mf}$ is the absorption coefficient due to exogenous fluorophore; $\mu'_{sx,m}$ is the reduced scattering coefficient; ω is the modulation frequency; ϕ is the quantum efficiency of the fluorophore, and finally, τ is the fluorophore lifetime associated with first order fluorescence decay kinetics. These equations are complemented by Robin-type boundary conditions on the boundary $\partial\Omega$ of the domain Ω modeling the NIR excitation source:

$$2D_x \frac{\partial u}{\partial n} + \gamma u + S(\mathbf{r}) = 0, \qquad 2D_m \frac{\partial v}{\partial n} + \gamma v = 0, \quad (3)$$

where n denotes the outward normal to the surface and γ is a constant depending on the optical reflective index mismatch at the boundary. The complex-valued function $S(\mathbf{r})$ is the excitation boundary source. The goal of fluorescence tomography is to reconstruct the spatial map of coefficients $\mu_{axf}(\mathbf{r})$ and/or $\tau(\mathbf{r})$ from measurements of the complex emission fluence v on the boundary. In this work we will focus on the recovery of only $\mu_{axf}(\mathbf{r})$. For notational brevity, we set $q = \mu_{axf}$ in the following paragraphs.

We have previously proposed a novel fluorescence tomography algorithm utilizing adaptive finite element methods [4]. In the following, we briefly describe the formulation of the scheme and its application to image reconstructions from multiple area illumination sources. M different area excitation light sources ($S^i(\mathbf{r}), i = 1, 2..M$) are employed to excite the embedded fluorophore in the phantom. Fluorescence measurements are taken on the illumination plane. The fluorescence image reconstruction problem is posed as a constrained optimization problem wherein an L_2 norm based error functional of the distance between boundary fluorescence measurements $\mathbf{z} = \{z^i, i = 1, 2...m\}$ and the diffusion model predictions $\mathbf{v} = \{v^i, i = 1, 2....m\}$ is minimized by variation of the parameter q, with the additional constraint that the coupled diffusion model corresponding to each illumination source ($A^i(q, [u^i, v^i]) = 0$) is satisfied. In a function space setting this minimization problem reads as:

$$\min_{q,\mathbf{u},\mathbf{v}} \; J(q, \mathbf{v}) \quad (4)$$

$$\text{subject to} \quad (5)$$

$$A^i(q; [u^i, v^i])([\zeta^i, \xi^i]) = 0, \qquad i = 1, 2...M. \quad (6)$$

Here, the error functional $J(q, \mathbf{v})$ incorporates a least square error term over the measurement part Γ of the boundary $\partial\Omega$ and a Tikhonov regularization term:

$$J(q, \mathbf{v}) = \sum_{i=1}^{i=m} \frac{1}{2} \left\| v^i - z^i \right\|_\Gamma^2 + \beta r(q), \quad (7)$$

β is the Tikhonov regularization parameter. The constraint $A^i(q; [u^i, v^i])([\zeta^i, \xi^i]) = 0$ is the weak or variational form of the coupled photon diffusion equations in frequency domain with partial current boundary conditions for the i^{th} excitation

source, and with test functions $[\zeta, \xi] \in H^1(\Omega)$:

$$A^i(q;[u^i,v^i])([\zeta^i,\xi^i]) =$$
$$(D_x\nabla u^i,\nabla\zeta^i)_\Omega + (k_x u^i,\zeta^i)_\Omega + \frac{\gamma}{2}(u^i,\zeta^i)_{\partial\Omega} + \frac{1}{2}(S^i,\zeta^i)_{\partial\Omega}$$
$$+(D_m\nabla v^i,\nabla\xi^i)_\Omega+(k_m v^i,\xi^i)_\Omega+\frac{\gamma}{2}(v^i,\xi^i)_{\partial\Omega}-(\beta_{xm}u^i,\xi^i)_\Omega$$

The solution of minimization problem (4) is determined as a stationary point of the Lagrangian [4, 5]

$$L(x) = J(q,\mathbf{v}) + \sum_{i=1}^{i=m} A^i(q;[u^i,v^i])([\lambda_i^{ex},\lambda_i^{em}]). \qquad (8)$$

Here, $\lambda_i^{ex}, \lambda_i^{em}$ are the Lagrange multipliers corresponding to the excitation and emission diffusion equation constraints for the i^{th} source, respectively, and we have introduced the abbreviation $x = \{\mathbf{u}, \mathbf{v}, \boldsymbol{\lambda}^{ex}, \boldsymbol{\lambda}^{em}, q\}$ for simplicity. A stationary point of $L(x)$ is found using the Gauss-Newton method wherein the update direction $\delta x_k = \{\delta\mathbf{u}_k, \delta\mathbf{v}_k, \delta\boldsymbol{\lambda}_k^{ex}, \delta\boldsymbol{\lambda}_k^{em}, \delta q_k\}$ is determined by solving the linear system

$$L_{xx}(x_k)(\delta x_k, y) = -L_x(x_k)(y) \qquad \forall y, \qquad (9)$$

where $L_{xx}(x_k)$ is the Gauss-Newton approximation to the Hessian matrix of second derivatives of L at point x_k, and y denotes the possible test functions. These equations represent one condition for each variable in δx_k. Once the search direction is computed from Eq. (9), the actual update is determined by calculating a safeguarded step length α_k:

$$x_{k+1} = x_k + \alpha_k \delta x_k. \qquad (10)$$

The step-length α_k can be computed from one of several methods, such as the Goldstein-Armijo backtracking line search [6]. The Tikhonov regularization term $\beta r(q) = \beta \|q\|_2^2$ added to the minimization functional $J(q, v)$ defined in Eq. (7) is used to control illposedness of the inverse solution. The Gauss-Newton equations are discretized by the finite element method. State and adjoint variables u, v, λ^{ex}, and λ^{em} are discretized and solved for on a mesh with continuous finite elements, while the unknown parameter map q is discretized on a separate mesh with discontinuous finite elements. Whenever Gauss-Newton iterations on these meshes have reduced the error function by a factor of 10^{-3} or the Gauss-Newton step length returned by the line search algorithm has fallen below 0.15, both meshes are refined using *a posteriori* refinement criteria [4]. Traditional optical tomography schemes utilize only one finite element mesh for the solution of diffusion equations corresponding to different illumination sources realized via fiber optics, while finite element simulations for multiple illumination sources in a non-contact area illumination mode have not been reported in literature till date. Simulation of photon transport via area excitation illumination requires careful finite element mesh design to capture the photon fluence variation in the tissue media. For multiple area illumination sources, optimal meshes can be obtained if the simulations corresponding to different sources are run on separate finite element meshes which are tailored to the illumination source being simulated. This task can be performed efficiently on multiprocessor computers or workstation clusters, wherein each source can be simulated on a separate compute node. The parallelization of Gauss-Newton equations is aided by the fact that measurements and diffusion equations for different area illumination cases are independent of each other and coupled only by the common set of unknown parameters q. The computations are implemented in an object oriented C++ based programming framework developed by Wolfgang Bangerth [6] with the help of open source deal.II finite elements library [7].

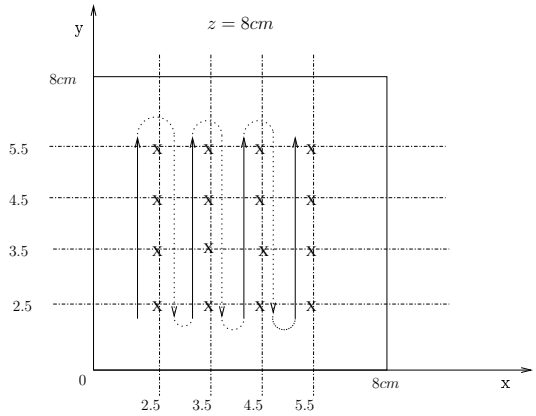

Fig. 2. Scanning gaussian source positions are indicated by 'X' on the illumination plane $z = 8$.

3. IMAGE RECONSTRUCTION SIMULATIONS

In this section non-contact fluorescence tomography with multiple excitation sources will be demonstrated. Synthetic measurements were generated on a 512 ml cubical tissue phantom with optical properties of 1% Liposyn. In a right handed coordinate system with the origin at the vertex of the phantom, $z = 8$ plane was set as the illumination and detection plane. Modulated($100MHz$) excitation light was delivered on the illumination plane via 16 gaussian sources scanning the surface(Fig-2). Three fluorescent targets ($5mm$ diameter spheres filled with $1\mu M$ Indocyanine Green solution in 1% liposyn) were simulated at a depth of $1cm$.

The additional computation burden introduced by employing multiple excitation illumination patterns was reduced by implementing the fluorescence tomography scheme in a parallel mode, wherein the forward and adjoint calculations for individual excitation sources were executed on separate threads, which were distributed on a linux Beowulf cluster with 32 $2.2GHz$ Opteron 64-bit processors and $4GB$ of memory per

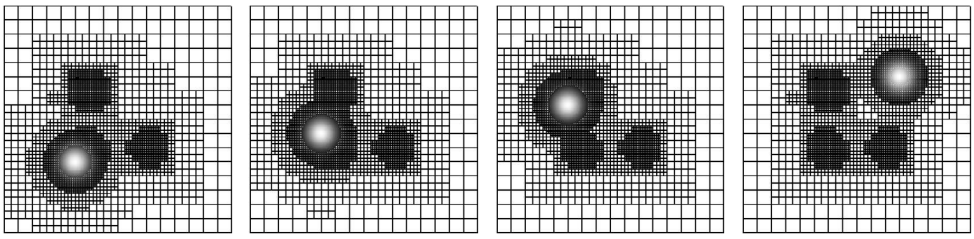

Fig. 3. Adaptively refined forward solution meshes: 1^{st}, 2^{nd} and 16^{th} sources are illustrated

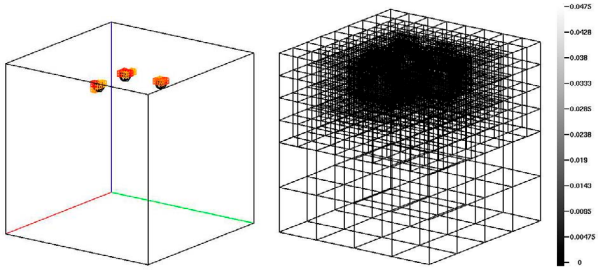

(a) (b)

Fig. 4. Three target reconstructions. Top 10% of the contour levels of fluorescence absorption are depicted. Black wireframes represent the true target locations, while the colored blocks represent the reconstructed targets

processor. Gauss-Newton iterations were started on coarse uniform discretizations for both forward and inverse meshes. Forward mesh consisted of 16^3 elements, while the initial parameter mesh was one level coarser with 8^3 elements. The forward meshes were adaptively refined to resolve the sharp gradients in excitation and emission fluence. The excitation fluence solution on the illumination plane is illustrated in Fig.3 along with the adaptively refined meshes for a set of sources. Fig.4 depicts the reconstructed image of three $1cm$ deep fluorescent targets. The final parameter mesh was adaptively refined around the three fluorescent targets and consisted of 4215 elements.

4. CONCLUSION AND FUTURE IMPLICATIONS

We have demonstrated a novel fluorescence optical tomography framework for recovering the location of multiple fluorescence targets embedded in tissue, from time dependent, non-contact boundary fluorescence measurements generated by multiple area excitation illumination sources. Like fiber optic based point illumination and detection schemes, multiple area illumination patterns enable wide spatial sampling of the tissue surface, while enabling the acquisition of dense measurement datasets and enhancing excitation light penetration in the tissue, with the resulting gains in sensitivity to low volume fluorescent targets. Adaptive mesh refinement based fluorescence tomography schemes are essential to generate optimal and efficient finite element meshes for recovering the fluorescent targets in clinically relevant situations, wherein large ($> 100cm^2$) tissue surface may need to be sampled, and no *a priori* information about the fluorescent target locations is available.

5. REFERENCES

[1] Ralf B. Schulz et. al., "Experimental fluorescence tomography of tissues with noncontact measurements," *IEEE transactions on medical imaging*, 2004.

[2] Adam B. Milstein et. al., "Statistical approach for detection and localization of a fluorescing mouse tumor in a turbid medium," *Applied Optics*, 2005.

[3] R. Roy et. al., "Tomographic fluorescence imaging in tissue phantoms: A novel reconstruction algorithm and imaging geometry," *IEEE Transactions on Medical Imaging*, vol. 24, no. 2, pp. 137–154, 2005.

[4] A. Joshi et. al., "Adaptive finite element modeling of optical fluorescence-enhanced tomography," *Optics Express*, vol. 12, no. 22, pp. 5402–5417, Nov. 2004.

[5] G.S. Abdoulaev et. al., "Optical tomography as a PDE constrained optimization problem," *Inverse Problems*, vol. 21, pp. 1507–1530, 2005.

[6] W. Bangerth, *Adaptive Finite Element Methods for the Identification of Distributed Coefficients in Partial Differential Equations*, Ph.D. thesis, University of Heidelberg, 2002.

[7] W. Bangerth et. al., `deal.II` *Differential Equations Analysis Library, Technical Reference*, 2006, `http://www.dealii.org/`.